

# **HiSST: 4th International Conference on High-Speed Vehicle Science Technology** 22 -26 September 2025, Tours, France



# **Feasibility Analysis of the Ascent Trajectory of the Scramjet Hypersonic Experimental Vehicle**

F. Fruncillo<sup>1</sup>, A. Vitale<sup>1</sup>, F. Cascone<sup>1</sup>, M. Marini<sup>1</sup>, S. Di Benedetto<sup>1</sup>, M. Albano<sup>2</sup>, R. Bertacin<sup>2</sup>

#### **Abstract**

The Italian Aerospace Research Centre and the Italian Space Agency are developing a Scramjet Hypersonic Experimental Vehicle, with the aim to design and test in flight enabling technologies for the implementation of the future transportation systems at hypersonic speed. The experimental mission envisages an air-launched solution, composed by a subsonic carrier that releases a rocket-based launch system, which is in charge of delivering the hypersonic vehicle to its experimental window. Flight mechanics analyses play a fundamental role in the design of the mission, the launch system and the experimental vehicle. This paper presents the flight mechanics analyses performed to assess the feasibility of the ascent leg of the mission performed by the launch system. It describes the methodology applied to assess the launch system flying qualities and to define its nominal trajectory. The paper highlights the challenges to be faced with in executing such analyses and discusses the obtained results which provide useful information concerning system configuration and mission definition and confirm the feasibility of the flight test.

Keywords: hypersonic vehicle, flight mechanics, scramjet, trajectory optimization, trim-ability

### **Nomenclature**

C<sub>lp</sub> – damping moment derivative

 $C_{L_{\alpha}}$  – lift coefficient derivative

 $C_{m\alpha}$  – pitching moment coefficient derivative

 $C_{n\beta}$  – yawing moment coefficient derivative CoG – Centre of Gravity

I<sub>x</sub> – moment of inertia about longitudinal axis

J – objective function L - rolling moment

L<sub>p</sub> – damping rolling moment

L<sub>0</sub> – driving rolling moment

LV – Launch Vehicle

M - Mach number

MAC - Mean Aerodynamic Chord

M<sub>y</sub> – total pitching moment

SHEV - Scramjet Hypersonic Experimental

Vehicle

SM - Static Margin

T - thrust

h – altitude

t - time

p - roll rate

 $\dot{p}$  – roll acceleration

x - state vector

 $\alpha$  – angle of attack

 $\beta$  – angle of sideslip

 $\delta_e$  – elevon deflection

 $\delta_T$  – thrust deflection

 $\Phi$  – roll angle

 $\psi$  – track angle

 $\gamma$  – flight path angle

 $\sigma$  – bank angle

### 1. Introduction

The Italian Aerospace Research Centre and the Italian Space Agency are developing a Scramjet

HiSST-2025-282 Page | 1 Feasibility Analysis of the Ascent Trajectory of the Scramjet Hypersonic Experimental Vehicle Copyright © 2025 by authors

<sup>&</sup>lt;sup>1</sup> Italian Aerospace Research Centre (CIRA), Via Maiorise 81043, Capua (CE), Italy, f.fruncillo@cira.it, a.vitale@cira.it, s.dibenedetto@cira.it, m.marini@cira.it

<sup>&</sup>lt;sup>2</sup> ASI, Italian Space Agency, 00133 Rome, Italy, marta.albano@asi.it, roberto.bertacin@asi.it

Hypersonic Experimental Vehicle (SHEV), with the aim to design and test in flight enabling technologies for the implementation of the future transportation systems at hypersonic speed, which will allow dramatically reducing travel times on long haul routes. Indeed, the availability of hypersonic aircraft offers several advantages both in civil and military applications, but their design also poses significant challenges related to heat, propulsion, and control at very high speeds. Flight mechanics help facing with these challenges, providing analyses and data that support the definition of the configurations of experimental vehicle and launch vehicle, and the assessment of the mission feasibility.

The flight test of the SHEV envisages an air-launched solution, composed by a subsonic carrier that releases a rocket-based launch system. The latter is in charge of delivering the SHEV to its experimental window. The flight mechanics analyses of the SHEV after its delivery to the experimental window have been already discussed in [1]. This paper presents the analyses of the ascent leg of the mission performed by the payload, defined as the SHEV connected to a launch vehicle (LV). Specifically, the paper describes the assessment of the trim and stability properties of the payload, and the definition of its nominal trajectory from the subsonic carrier separation till to the delivery of the SHEV within the experimental window. The LV is a solid propellant booster equipped with thrust vectoring system and two elevons to trim and manoeuvre. Therefore, the trim computation shall manage the availability of two redundant controls with respect to pitch axis rotation, that is, the aerodynamic control surfaces and the thrust vectoring. Moreover, the thrust contributes to the pitching moment and its intensity is time varying along the trajectory; it shall be taken into account in the trim, although the computation is performed on the whole flight envelope independently from the time. The most promising configuration of the payload poses the experimental vehicle upside down under the launch vehicle, thus requiring specific roll manoeuvres to reach the experimental flight conditions of the SHEV. The feasibility of such manoeuvres shall be assessed in the nominal trajectory computation. The sizing of the booster is another output of the trajectory design, because it depends on the thrust required to achieve the desired final altitude and velocity. The following sections of this paper first describe the mission concept and payload configuration (section 2), and next present the flight mechanics analyses methodologies (section 3) and results (section 4). Finally, a conclusions section ends the paper.

# 2. Mission and system definition

### 2.1. Experimental mission concept

The preliminary mission concept envisages an air-launched solution with a carrier (stage I) capable of releasing the payload at a target point (Sep1) defined in terms of speed and altitude. After Sep1, the launch vehicle accelerates until it reaches the experimental window and releases the hypersonic demonstrator (Sep2). Both separation conditions are listed in Table 1. Next, the scramjet on board the demonstrator turns on and operates for at least 10 seconds; the demonstrator shall perform a hypersonic flight at constant altitude, guaranteeing a positive aero-propulsive balance and aerodynamic efficiency in the range 3÷4. Finally, the scramjet shuts off, and the demonstrator glides decelerating until the vehicle becomes uncontrollable and splashes down. The mission concept is graphically described in Fig 1.

Table 1. Separation conditions

Separation	Altitude [Km]	Mach
Sep1	13.5 ÷ 15	0.6
Sep2	27 ÷ 32	6 ÷ 8

Note that it is assumed that the carrier returns back and lands at the airport, whilst both the launch vehicle and the hypersonic propelled demonstrator are disposable vehicles, thus they are not recovered.

### 2.2. System configuration

Several configurations of the system composed by launch vehicle and flight demonstrator have been examined with the aim to quarantee high aerodynamic efficiency and low structural loads, and to simplify the structural interface between the launch vehicle and the SHEV, in order to reduced integration complexity and separation's risks when the SHEV is released.

Two main structural configurations were analysed, one where the SHEV and launch vehicle are in line

and another where the SHEV is positioned under the launch vehicle (see Fig 2). For these two configurations, different solutions for joint SHEV and launch vehicle have been evaluated with different types of fixing. The feasibility studies are supported by preliminary stress analysis calculation, which identified as most promising configuration the one in which the experimental vehicle is fixed upside down under the launch vehicle.

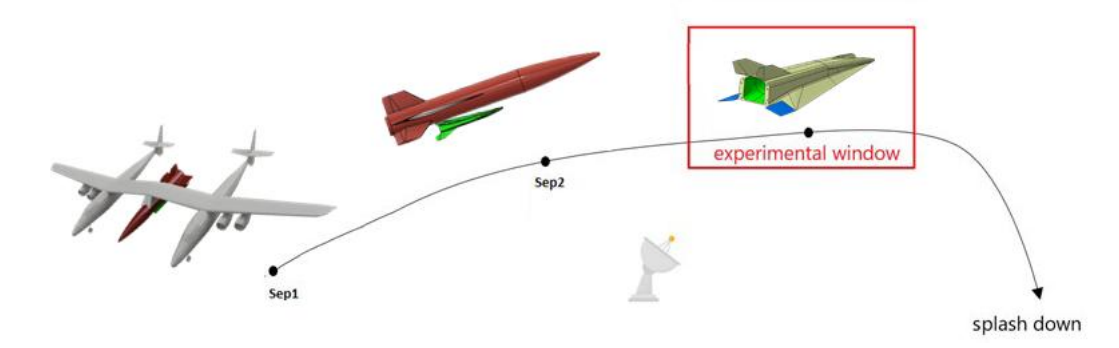


Fig 1. Graphical representation of the experimental mission concept

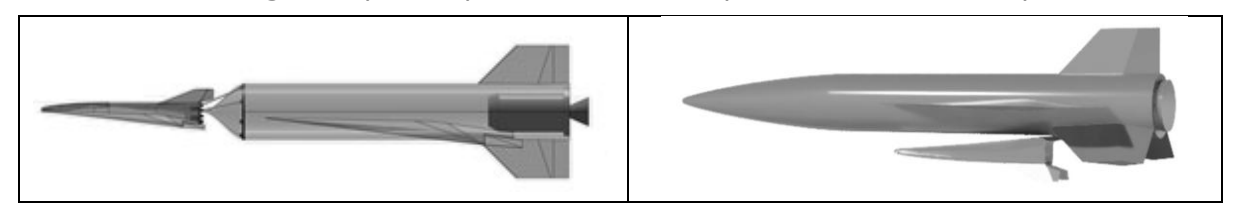


Fig 2. Examined structural configurations of the payload: SHEV and launch vehicle in line (left) and SHEV under launch vehicle (right)

# 3. Flight mechanics methodology

Flight mechanics analyses aim to assess the payload flying qualities and to define its nominal trajectory. The analyses examined the most promising configuration, that is, the ones with the SHEV under the launch vehicle. In details, the following activities were carried out:

- Evaluation of the payload longitudinal trim capability, guaranteed by the exploitation of aerodynamic control surfaces and thrust vectoring, on the whole flight envelope, defined by Mach number, angle of attack, altitude (which affects aerodynamic viscous effect), and for the whole range of possible centre of gravity (CoG) positions; the analysis produces the trimmed aerodynamic database and the trimmable envelope, that is, the minimum and maximum admissible angle of attack for each value of the other three independent variables (Mach, altitude, CoG).
- Computation of the longitudinal nominal trajectory able to track a reference flight path angle profile and to reach the required final conditions (experimental window altitude and Mach number), through an optimization process.
- Assessment of the feasibility and effects of the 180 degrees roll manoeuvre, required to set the SHEV to the experimental window attitude; this analysis identifies the best suitable flight conditions along the longitudinal nominal trajectory to perform the manoeuvre, assesses the feasibility of the manoeuvre, and computes, through a simplified and de-coupled model, the roll dynamics.
- Computation of the complete nominal trajectory, taking into account the execution and the effects of the roll manoeuvre dynamics.
- Assessment of the static stability along the obtained nominal trajectory.

The first two bullets are executed for different values of the thrust intensity and corresponding payload weight, and the best solution in terms of achieving the required final conditions is selected. This process allows to dimension the size of the launch vehicle's booster. The methodologies applied to perform each of the above listed steps are described in the following sub-sections.

### 3.1. Trim

Rotational trim is the condition in which the resulting moment acting on the vehicle is null. Since the payload mission is almost purely longitudinal (except for few seconds in which the system performs a roll manoeuvre), the longitudinal trim is evaluated, which is related to null pitching moment.

Two forces act on the system and produce moment, the aerodynamics and the propulsion ones. The aerodynamic database provides the aerodynamic coefficients as composed of the inviscid contribution, function of Mach number (M), angle of attack ( $\alpha$ ) and aerodynamic surfaces deflection ( $\delta_e$ ), and the viscous correction, which depends on the Reynolds number, through the altitude (h), and Mach number. The inviscid terms are further split in clean contribution (null elevons deflection) and elevons contribution. The elevons deflection can be used to control the aerodynamic forces and moment; the payload in clean configuration tends to pitch down, therefore an upward deflection (negative) of the elevons is required to null the total pitching moment. The thrust force is time varying according to a predefined profile, as shown in Fig 3. It is not aligned to the CoG, thus contributing to the pitching moment, Moreover, the fuel consumption produces a variation of the CoG position during the flight, which also affects the trim computation. It is worthy to note that except for the very last seconds of the thrust time profile, in which the intensity goes quickly to zero, the minimum value of the thrust is obtained at the beginning of the trajectory, when the booster switches on. The thrust vectoring capability ( $\delta_T$ ) allows to manage the moment produced by this force.

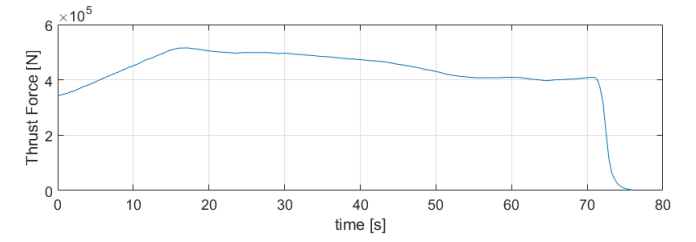


Fig 3. Thrust force time history

Based on the above description, this trim problem presents two peculiarities:

- two independent control variables are available to null the pitching moment, that is, elevons deflection and thrust vectoring angle; therefore, a control allocation strategy shall be applied;
- the thrust gives a contribution to the pitching moment which is time varying along the trajectory.

The solution of the trim problem in each point of the flight envelope  $(M, \alpha, h)$  and for each CoG position, can be formulated as follows

$$\exists \delta_{e_{Trim}} \in \left[\delta_{e_{min}}, \delta_{e_{max}}\right] \ and \ \exists \delta_{T_{Trim}} \in \left[\delta_{T_{min}}, \delta_{T_{max}}\right]$$
 such that 
$$M_{y}(M, \alpha, h, CoG, \delta_{e_{Trim}}, T, \delta_{T_{Trim}}) = 0 \tag{1}$$

where  $\textit{M}_{\textit{y}}$  is the global (aerodynamic plus thrust) pitching moment, T is the thrust,  $\left[\delta_{e_{min}}, \delta_{e_{max}}\right]$  and  $[\delta_{T_{min}}, \delta_{T_{max}}]$  define the allowable ranges of variation for elevons deflection and thrust vectoring angle, respectively: the other parameters have been already defined. The problem is solved by computing the elevons deflection that satisfies eq. (1), while the thrust is assumed constant to its initial minimum value. The solution is determined for each flight condition  $(M, \alpha, h, CoG)$  and for each thrust vectoring angle which varies within its allowable range. Thus, the trim elevons deflection is a function depending on five independent variables. It can be reduced to four-dimensional function if we consider for each flight condition  $(M, \alpha, h, CoG)$  only the trim corresponding to the maximum or the minimum of the absolute value of thrust vectoring deflection that quarantees the trim. These choices allow maximizing the use of one control to trim and exploiting the other control mainly for manoeuvring purpose. Of course, different and optimized allocation between thrust vectoring and elevons deflection can be applied, the proposed ones only allow to assess the mission feasibility. In each flight condition where trim exists, the aerodynamic lift and drag coefficients corresponding to the trim elevons deflection are evaluated and the results constitute the trimmed aero-database. It is worthy to note that due to the pithing down trend of the payload in clean configuration (with null deflection of both elevons and thrust vectoring), a negative angle of thrust vectoring (that is, thrust downward) is required to trim the system. With this approach, the contribution to the moment due to the propulsion in each flight condition is computed considering the initial value of the thrust and a nominal thrust deflection angle needed to trim; along the trajectory, the actual value of the thrust is different from the initial one, and consequently the actual value of the thrust vectoring angle needed to trim is different from the nominal one. The actual trim angle is computed by solving the equation in which the pitching moment due to the initial thrust and related nominal trim angle is equated to the moment due to actual thrust and actual thrust vectoring trim angle. Since the actual thrust is always bigger than the initial one, the module of the actual thrust vectoring angle will result lower than the nominal one.

Finally, for each triple (M, h, CoG) it is possible to compute the minimum and maximum values of the angle of attack which limit the range where the system is trimmable, that is, the trimmable envelope. The obtained four-dimensional trimmed aero-database and three-dimensional trimmable envelope are used to compute the nominal trajectory.

## 3.2. Longitudinal nominal trajectory

The definition of the longitudinal nominal trajectory consists in computing the guidance law of the vehicle, which for a longitudinal mission coincides with the angle of attack profile. Next, this profile is used as input to a simulation model to obtain the time histories of the vehicle's state vector and all the parameters that are relevant for mission analysis. The computation of the guidance law requires the solution of the following nonlinear constrained optimization problem:

$$\min_{\alpha} J$$
such that
$$\begin{cases}
\dot{x}(t) = F(\alpha(t), x(t), t) \\
\alpha_{min}(M, h, CoG) \leq \alpha(M, h, CoG) \leq \alpha_{max}(M, h, CoG)
\end{cases}$$
(2)

The objective function J is selected based on the mission requirements. The mission concept requires that the system reaches the SHEV experimental window defined by altitude and Mach number. Therefore, J is computed as summation of two terms: the RMS error with respect to a flight path angle reference profile that leads to the required altitude, and the absolute error with respect to the target final Mach number. Concerning the constraints, the first equation represents the translational dynamics, in which the vehicle is considered as a three degrees of freedom point mass in trimmed aerodynamic conditions, moving around a spherical non-rotating Earth within a standard atmosphere in stationary (null winds) state [2]. In the equation, x denotes the vehicle state vector, and F is the function that expresses the state vector derivatives depending on state vector and controls (angle of attack). The inequality constraint identifies the admissible range of variation for the angle of attack, bounded by  $\alpha_{min}$  and  $\alpha_{max}$ , that guarantees good flyability properties, as computed in the trim analysis. The angle of attack profile is defined through nodal points with respect to Mach number values, which increase monotonically during the mission; the variation of  $\alpha$  between two nodal points is assumed linear. The computation of the angle of attack values in the nodal points is carried out numerically, by using the MATLAB minimization routine "fmincon" [3] and an active-set strategy [4]. Due to the presence of local minima, the problem solution depends on the initial guess; several guesses are used and the one corresponding to the best solution (minimum objective function) is selected.

Both trim analysis and longitudinal trajectory computation are performed for the nominal thrust profile and for different thrust profiles obtained scaling the nominal one. The minimum scale factor that guarantees the satisfaction of mission requirement is used to size the system booster.

### 3.3. Roll manoeuvre

In order to release the SHEV in the required attitude within the experimental window, it is necessary to perform a roll manoeuvre during the ascent trajectory. The manoeuvre is executed in flight condition which allow assuming that it is of pure roll motion around the longitudinal axis of the system. Furthermore, to avoid the effects that thrust would have if it was not aligned with the longitudinal axis during the manoeuvre, it must be performed under zero thrust-vectoring conditions. Assuming negligible linear and angular velocities along the y and z axes, the roll dynamics can be described by the Euler equation [5]

$$I_{r}\dot{p} = L \tag{3}$$

where  $I_x$  is the moment of inertia about the longitudinal axis (which varies throughout the trajectory), p is the roll rate, and L the rolling moment. In particular, the latter can be decomposed as  $L = L_0 + L_0$  $L_p p_r$ , i.e., into a driving  $(L_0)$  and a damping  $(L_p p)$  component. Starting from the longitudinal trim conditions established in the previous section, the driving moment is generated via anti-symmetric deflection of the left and right elevons: by opening in opposite directions, i.e.,  $\delta_e = \delta_{e_{Trim}} \pm \Delta_e$ , they preserve the longitudinal trim balance, while inducing the required aerodynamic rolling moment. Its magnitude therefore depends on the angle of attack, Mach number, altitude (through the viscous effect), and the CoG position at the instant of manoeuvre. Regarding the damping contribution, it can be written in terms of the damping moment derivative  $C_{l_n}$ , that is a function of angle of attack and Mach number, and is obtained from aerodynamic simulations. The surfaces deflection required is set to track a step profile of the roll angle from  $0^{\circ}$  to  $180^{\circ}$ , obtained by time integration of the roll rate p. A PID controller has been tuned to ensure accurate tracking of this reference profile. The Simulink block diagram of the closed loop simulation environment is shown in Fig 4. To maintain consistency with the pure roll assumption, the manoeuvre is performed at trajectory points where the angle of attack is close to zero. In particular, different trim conditions along the trajectory were examined to evaluate manoeuvre performance in terms of execution time and recovery from any overshoot generated in tracking the roll angle.

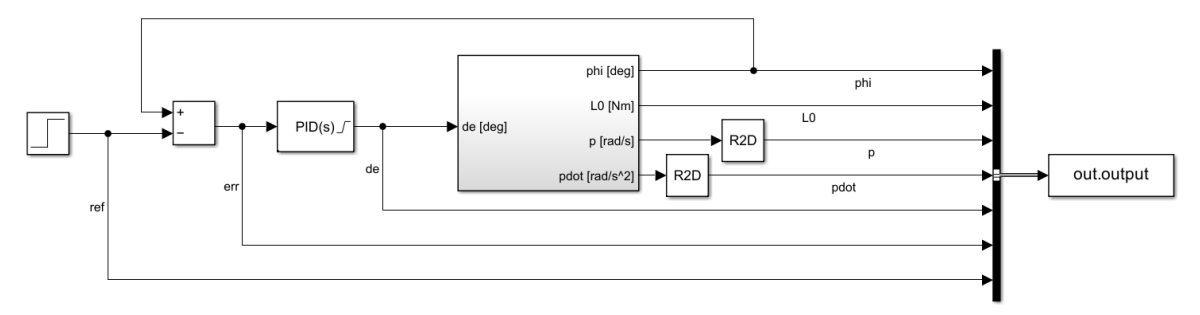


Fig 4. Simulink block diagram of closed loop roll dynamics

## 3.4. Nominal trajectory

The nominal trajectory is composed of the three degrees of freedom translational motion of the centre of gravity of the system and the effect of the roll manoeuvre. This manoeuvre can be performed:

- at the beginning (soon after the release from the carrier) or at the end (just before the SHEV release) of the system trajectory, when the booster is switched off
- in an intermediate point of the system trajectory, in which the commanded angle of attack is close to zero and the booster is on.

A different methodology is applied in each case to compute the nominal trajectory. In the first case, the trajectory is split in two legs, the boosted one, in which the computation is performed as described in section 3.2, and the unpropelled one, in which the roll manoeuvre is performed in free fall. In the latter leg, the trajectory is obtained by solving the equations of dynamics when they are fed with the following inputs:

- null thrust
- null angle of attack
- predefined bank angle profile.

The null angle of attack is imposed to make applicable the hypothesis of pure roll motion around the system longitudinal axis. Indeed, in this case the roll angle coincides with the bank angle, thus defining the bank angle time history as computed in section 3.3. After reaching about 180 degrees of bank angle, a negative angle of attack is applied for few seconds in order to execute a pull up and to reach a suitable flight path angle for the following mission phase (the system is upside down). In the second case, the whole trajectory is computed through the solution of the optimization problem defined in section 3.2 and the roll dynamics is included in the equation of motion, by assuming again that the roll angle coincides with the bank, which affects the direction of the lift. The bank dynamic is precomputed as in section 3.3 and provided as input to the point mass simulation model.

### 3.5. Static stability

The longitudinal static stability of the system is assessed through the following relations:

$$C_{m\alpha}(M,\alpha,h,CoG,\delta_{e_{Trim}},T,\delta_{T_{Trim}}) < 0$$
 (5)

$$SM = -\left(C_{m\alpha}(M, \alpha, h, CoG, \delta_{e_{Trim}}, T, \delta_{T_{Trim}}) / C_{L\alpha}(M, \alpha, h, CoG, \delta_{e_{Trim}})\right) > 0$$
 (6)

where  $C_{m\alpha}$  and  $C_{L\alpha}$  are the derivatives of the pitching moment and lift coefficients with respect to the angle of attack, respectively.  $\mathcal{C}_{m\alpha}$  is also denoted as pitch stiffness. SM is the static margin and represents the distance between the CoG and the neutral point, i.e., the position at which the vehicle would be neutrally stable. Therefore, a positive static margin quantifies how much the CoG can be shifted aft without compromising static stability in response to angle of attack perturbations. The stability parameters are numerically computed along the nominal trajectory.

## 4. Flight mechanics results

#### 4.1. Trim

Trim results are defined for each combination of Mach number, angle of attack, altitude, and centre of gravity position, both in the x and z directions of the longitudinal plane. The boundaries of the ranges considered for these four variables are listed in the following table.

Table 2. Flight envelope

Mach	Angle of attack [deg]	Altitude [km]	X coordinate CoG [m]	Y coordinate CoG [m]
0.6 ÷ 8	-24 ÷ 24	12 ÷ 34	7.92 ÷ 9.11	-0.27 ÷ -0.11

The positions of the CoG are expressed in construction axes, centred at the nose of the vehicle, with the x-axis pointing towards the tail and the z-axis running from the pilot's feet to head. The equilibrium elevon deflection maps obtained from the trim analysis are shown in Fig 5 for different combinations of the four governing variables. Specifically, the results are presented in the M  $-\alpha$  plane, for both low and high altitude conditions, and for forward and aft positions of the centre of gravity.

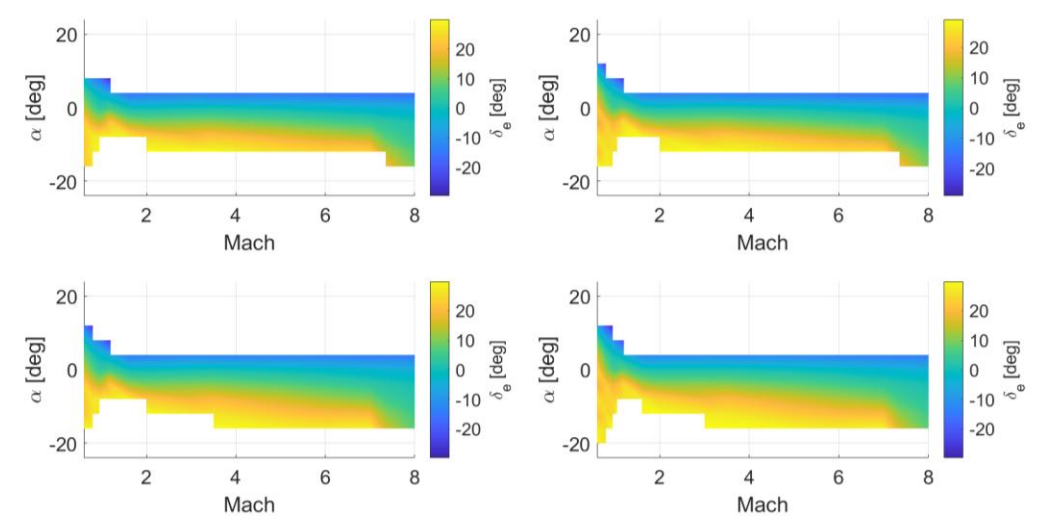


**Fig 5.** Elevons' deflections in M –  $\alpha$  plane: low altitude, forward CoG (left up); high altitude, forward CoG (right up); low altitude, aft CoG (left down); high altitude, aft CoG (right down)

From the trim maps, it can be observed that the effect of altitude is less significant than that of the CoG position. It is important to note that altitude-related effects are primarily due to viscous corrections in the aerodynamic model, which are more pronounced at low Mach and Reynolds numbers, that is, during the early part of the trajectory, when the vehicle is flying slowly and at low altitude. In contrast, the CoG position has a more substantial influence on trim capability, with improved trim margins when the CoG is located further aft, closer to the tail of the vehicle. In all plots, the most challenging region for achieving trim is consistently found in the transonic regime. It should be emphasized, however, that

HiSST-2025-282 Page |7 Copyright © 2025 by authors the vehicle does not encounter all the flight conditions represented in the maps. In particular, this is due to the fact that during the mission the CoG position and altitude are not independent. From the trim analysis, it is possible to derive maps of the minimum and maximum allowable angle of attack for each fixed combination of Mach number, altitude, and CoG position (both x and z). These values are essential during trajectory optimization, as they define the bounds within which the angle of attack can vary without compromising the vehicle's equilibrium. The results are shown in Fig 6, corresponding to the extreme cases of CoG positioning. These results further confirm that the transonic region is the most challenging for maintaining the vehicle's equilibrium.

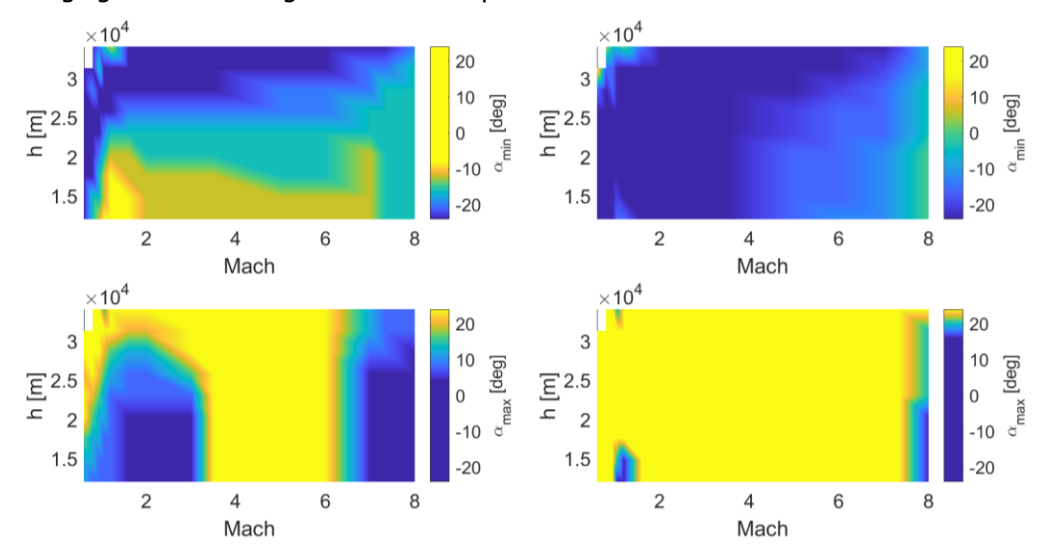


**Fig 6.** Angle of attack bounds in Mach – Altitude plane: minimum  $\alpha$ , forward CoG (left up); minimum  $\alpha$ , aft CoG (right up); maximum  $\alpha$ , forward CoG (left down); maximum  $\alpha$ , aft CoG (right down)

### 4.2. Longitudinal nominal trajectories

The optimization problem for the computation of the nominal longitudinal trajectory was solved for different sizes of the thrust, obtained scaling the nominal profile shown in Fig 3. Finally, 65% of original thrust is needed to reach the experimental window, and this value has been selected as sizing. The following figures describe the obtained trajectory, in which the controls remain within their allowable ranges and final Mach number and altitude are within the target ranges.

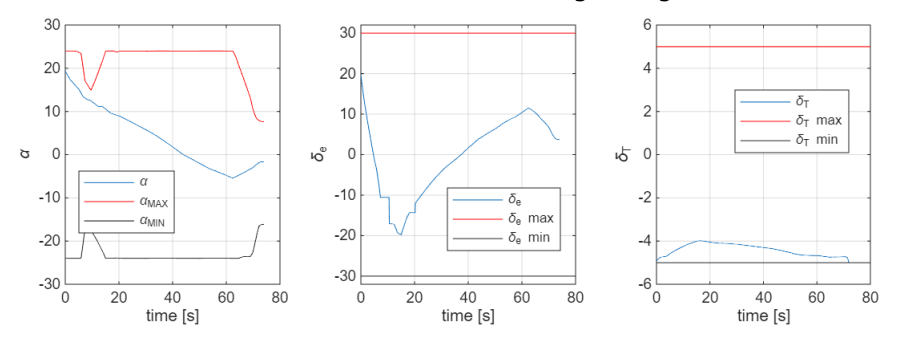


Fig 7. Longitudinal trajectory: commands histories

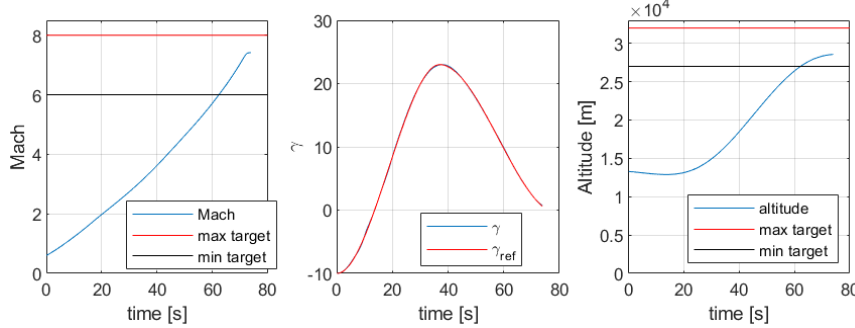


Fig 8. Longitudinal trajectory: Mach number (left), flight path angle (centre) and altitude (right)

The reference flight path angle profile is perfectly tracked, being the reference and the actual trajectories indistinguishable. It is worthy to note that after the separation from the carrier the payload is released horizontal at 13.5 km altitude, whereas the initial conditions considered in the optimization problem have a negative flight path angle (-10 degrees) and a lower altitude 13.287 km; it is due to 5 seconds of initial uncontrolled free fall (not shown in the figures), needed to guarantee the safe separation from the carrier.

### 4.3. Roll manoeuvre

Fig 9 shows the roll manoeuvre performed at three points of the ascent leg: beginning, middle, and end. In the first case, it is executed before firing the booster and before starting the guidance (assuming null angle of attack); the flight conditions are coincident with the release from the carrier. The second point is about 44s after the start of the guidance, when the angle of attack as computed for the longitudinal nominal trajectory is about zero (see Fig 7). Finally, the last point coincides with the final condition of the longitudinal nominal trajectory; also in this case, the booster is switched off and the angle of attack is assumed null during the roll execution.

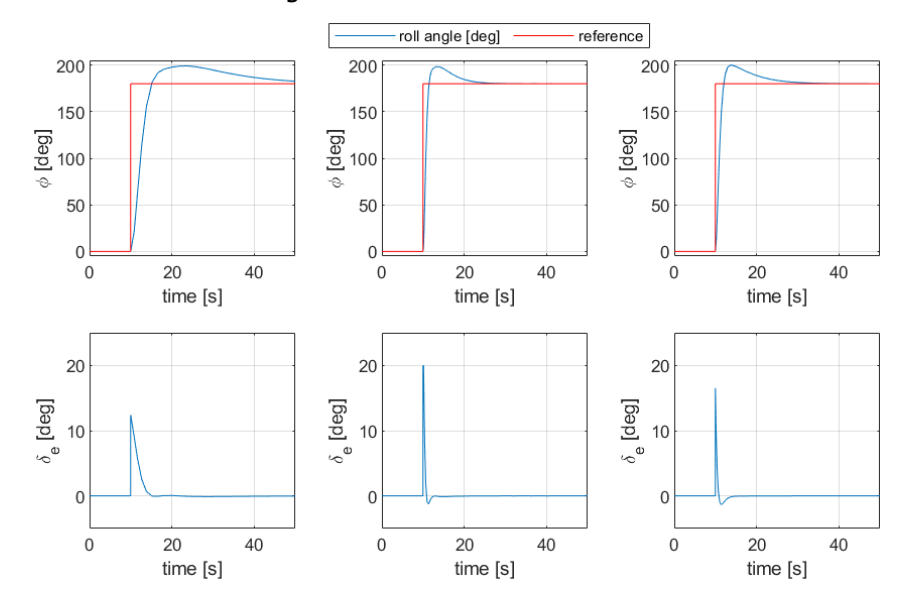


Fig 9. Roll dynamics (top row) and elevons deflection (bottom row) for roll manoeuvre performed at the beginning (left), middle (centre), and end (right) of the ascent leg

The roll angle  $(\Phi)$  dynamic is guite similar in the three manoeuvres, with a slightly longer transient in the first case. However, the time to achieve a 180-degree roll is just a few seconds, aligning with the roll performance characteristics expected of high-speed aircraft [6]. The required elevons deflection presents a maximum value of about 12 degrees in the first case and bigger values (however below 20 degrees) in the other two cases. For these latter cases, the elevons deflection required to trim is well below 10 degrees (see Fig 7), therefore the manoeuvre can be performed keeping the total elevons deflection within its allowable range, that is [-30, 30] degrees. For the first case, the deflection required to trim without using the thrust vectoring is already at the elevons bound, thus the deflection for the roll manoeuvre exceeds the allowable elevons deflection range; moreover, in this condition the system exhibits a slightly unstable longitudinal behaviour. However, some improvements (configuration, elevon deflection range, control design) could be considered. Regarding directional stability, the sign of the yawing moment derivative with respect to the sideslip angle, i.e.,  $C_{n\beta}$ , was evaluated at the initial instant of the roll manoeuvre and the system results directionally stable in all three scenarios considered. Specifically, the values of  $C_{n\beta}$  are 0.0126, 0.0036, and 0.0046, corresponding to the manoeuvre performed at the beginning, middle, and end of the trajectory, respectively.

## 4.4. Nominal trajectories

The following figures show the effect of the roll manoeuvre on the longitudinal trajectory. If the manoeuvre is performed at the beginning of the ascent leg (Fig 10 and Fig 11), the system experiences an initial fall at almost constant Mach number. To compensate for it, a higher release altitude from the carrier (14.5 km) is assumed. As soon as the bank reach 180 degrees, a pull up manoeuvre (negative

HiSST-2025-282 Page |9 Copyright © 2025 by authors angle of attack, due to upside down condition) is executed, in order to achieve acceptable initial flight path angle for the boosted phase. The angle of attack remains within its allowable range, as well as the thrust vectoring angle (not shown for the sake of brevity), the use of which for trim purpose during the boosted phase is minimized in this case. Elevons deflection exceeds for few seconds the minimum bound, during the roll manoeuvre. Final Mach number and altitude are within the target ranges. The reference flight path angle profile (defined only for the boosted phase) is perfectly tracked, being the reference and the actual trajectories indistinguishable.

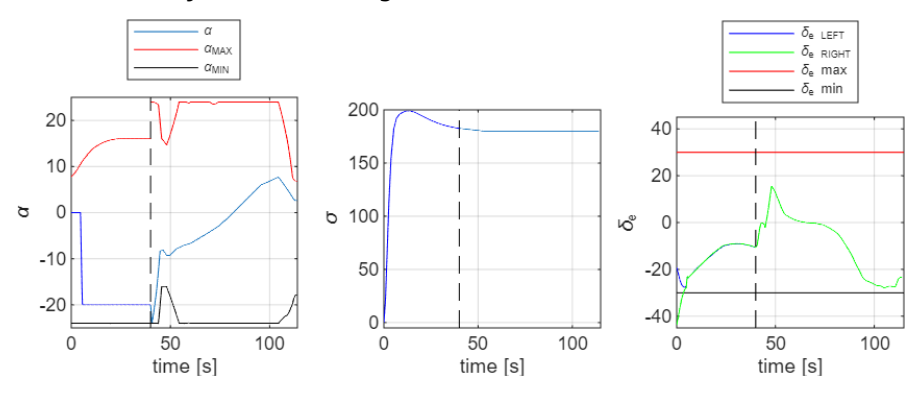


**Fig 10.** Initial roll: angle of attack (left), bank angle (middle), elevons deflection (right); the dotted line in the figures separates the roll manoeuvre phase (left) from the ascent phase (right)

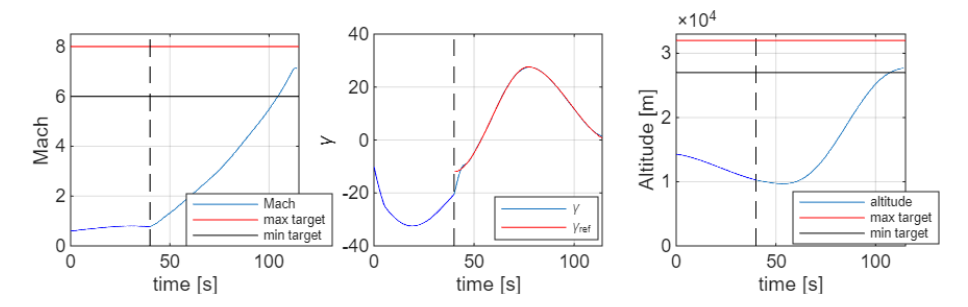


**Fig 11.** Initial roll: Mach number (left), flight path angle (middle), altitude (right); the dotted line in the figures separates the roll manoeuvre phase (left) from the ascent phase (right)

If the roll manoeuvre is executed in the middle of the ascent (Fig 12 and Fig 13), at 44 seconds after the start of the ascent leg, then the system does not experience any free fall, and the release altitude from the carrier is set at 13.5 km. All the constraints on angle of attack, elevons deflection, and final values of Mach and altitude are satisfied. Similar results hold for roll manoeuvre performed at the end of the ascent phase (Fig 14 and Fig 15). For both these cases the use of the thrust vectoring for trim purpose during the boosted phase is maximized; however, the thrust vectoring angle is always within the range  $-5 \div 0$  degrees.

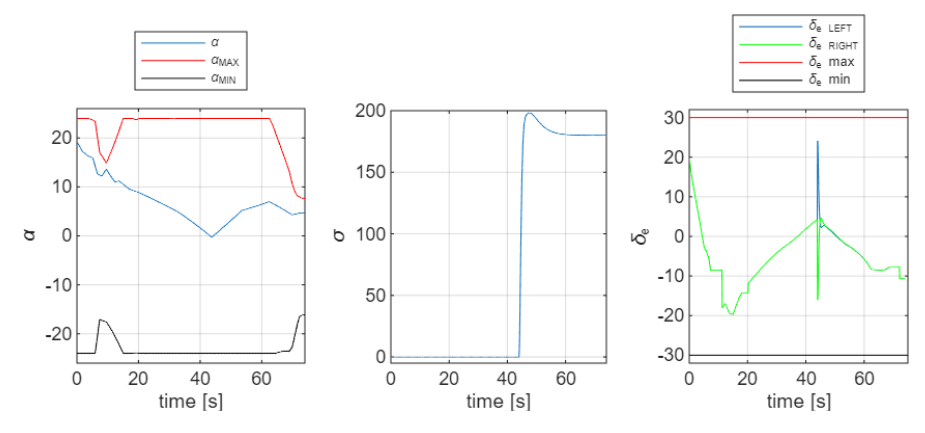


Fig 12. Intermediate roll: angle of attack (left), bank angle (middle), elevons deflection (right)

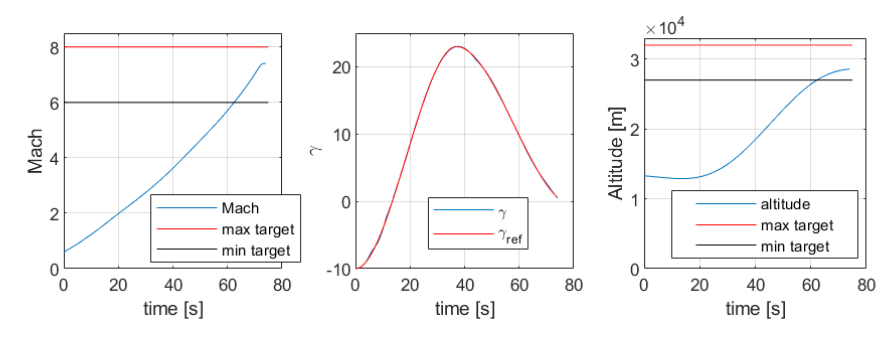


Fig 13. Intermediate roll: Mach number (left), flight path angle (middle), altitude (right)

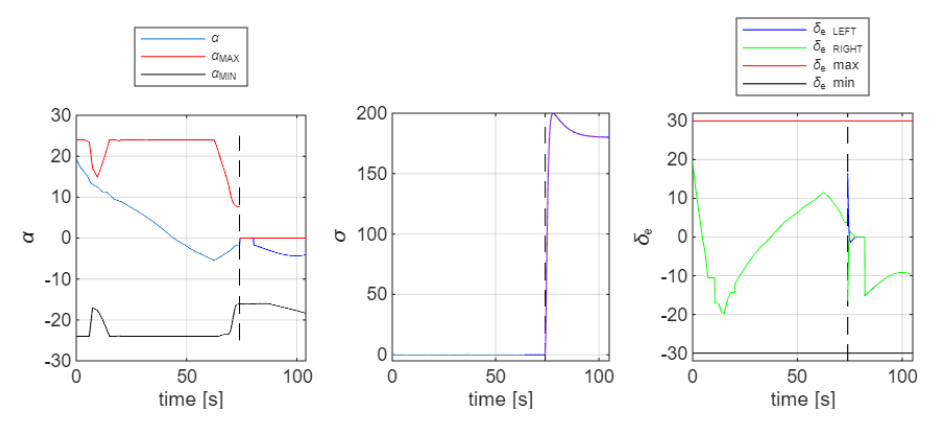


Fig 14. Final roll: angle of attack (left), bank angle (middle), elevons deflection (right); the dotted line in the figures separates the ascent phase (left) from the roll manoeuvre phase (right)

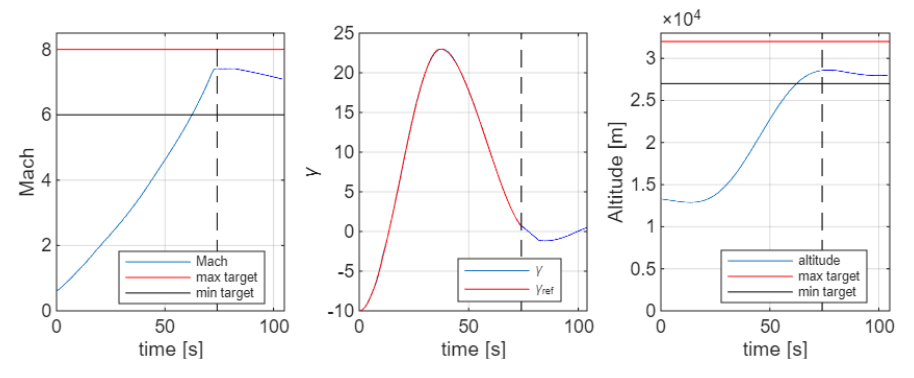


Fig 15. Final roll: Mach number (left), flight path angle (middle), altitude (right); the dotted line in the figures separates the ascent phase (left) from the roll manoeuvre phase (right)

# 4.5. Static stability

The derivatives of the pitching moment and lift coefficients with respect to the angle of attack are evaluated at trim conditions throughout the entire trajectory. Notably, the pitching moment derivative is sensitive to the CoG position, which varies over the course of the mission. The following plots show pitch stiffness and static margin.

Trajectories in which the roll manoeuvre is performed during the intermediate or final phases are always longitudinally stable. In contrast, when the manoeuvre is executed at the beginning of the trajectory, the vehicle exhibits a slightly unstable configuration.

HiSST-2025-282 Page |11

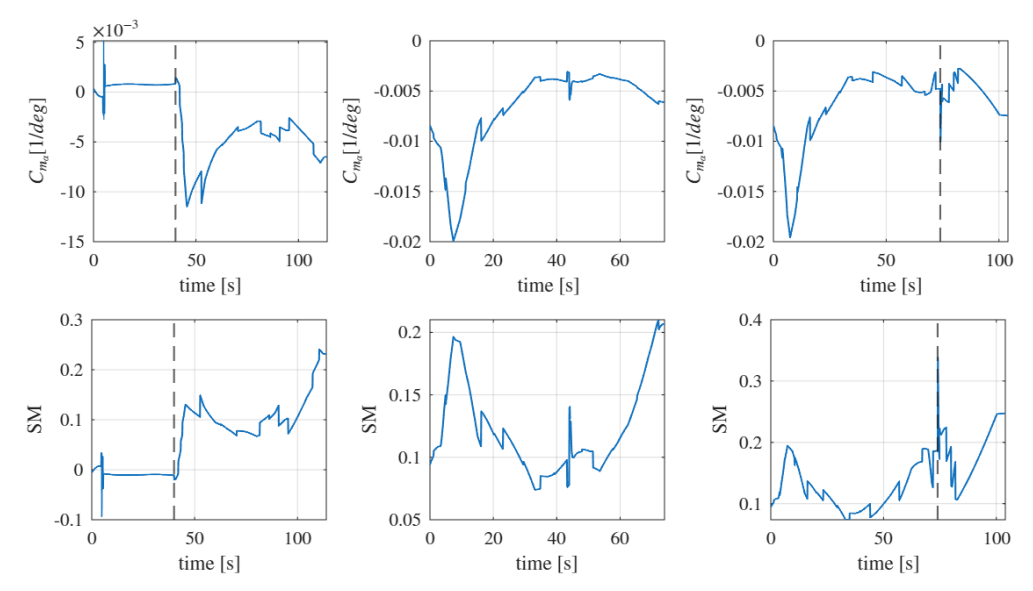


Fig 16. Pitch stiffness (top) and Static Margin (bottom) along the nominal trajectory for initial roll (left), intermediate roll (middle) and final roll (right); the dotted line in the figures for initial and final roll separates the ascent phase from the roll manoeuvre phase

### 5. Conclusions

This paper presented and discussed the flight mechanics analyses performed to support the preliminary design of the SHEV mission. The analyses concerned the assessment of the trim and stability properties, and the definition of the nominal trajectory of the mission payload, composed by a rocket-based launch vehicle and the SHEV demonstrator. The most promising configuration poses the demonstrator upside down under the launch vehicle, thus requiring specific roll manoeuvres to reach the experimental flight conditions. The nominal trajectory definition included the feasibility analysis of such manoeuvres and the sizing of the launch vehicle booster, based on the thrust required to achieve the desired final altitude and velocity.

The analyses highlighted good flying qualities of the system in the examined flight envelope, with most challenging conditions in transonic regime, as expected. Three nominal trajectories were computed, mainly differing for the flight conditions in which the roll manoeuvre is executed. They are compliant with all the applicable mission requirements and preliminary system constraints, with only one of them exhibiting a slightly unstable longitudinal behaviour during the roll manoeuvre (unboosted phase) and an elevons deflection needed to trim and manoeuvre which exceed the allowable bounds. A reduction of the thrust to 65% of the original dimensioning still allows achieving the SHEV experimental window; this outcome is exploited to size the booster. In general, the obtained results provide useful information concerning mission definition and confirm the feasibility of the flight test.

# **Acknowledgements**

The work has been co-funded by Italian Space Agency and CIRA ScPA in the frame of the agreement nr. 2022-13-HH.0-F43D22000410005.

### References

- 1. Vitale, A., Di Benedetto, S., Marini, M., Pizzurro, S., Bertacin, R.: Flyability Assessment and Trajectory Design for a Scramjet Hypersonic Experimental Vehicle. HiSST: 3rd International Conference on High-Speed Vehicle Science Technology, Busan, Korea (2024)
- 2. Vinh, N. X., Busemann, A., Culp, R. D.: Hypersonic and planetary entry flight mechanics. NASA Sti/Recon Technical Report A, 81, 16245 (1980)
- 3. Powell, M. J. D.: A Fast Algorithm for Nonlinearly Constrained Optimization Calculations. Numerical Analysis, ed. G. A. Watson, Lecture Notes in Mathematics, Springer-Verlag, Vol.

630 (1978)

- 4. Gill, P. E., Murray, W., Wright, M. H.: Practical Optimization. London, Academic Press (1981)
- 5. Regan, F. J.: Re-entry vehicle dynamics. AIAA (American Institute of. Aeronautics and Astronautics) Education Series, New York (1984)
- 6. Mitchell, D. G., Klyde, D. H., Pitoniak, S., Schulze, P. C., Manriquez, J. A., Hoffler, K. D., & Jackson, E. B. (2020). NASA's flying qualities research contributions to MIL-STD-1797C